Mitigating Thermoelastic Dissipation of Flexural Micromechanical Resonators by Decoupling Resonant Frequency from Thermal Relaxation Rate

Xin Zhou,[1] Dingbang Xiao,[1,*] Xuezhong Wu,[1] Qingsong Li,[1] Zhanqiang Hou,[1] Kaixuan He,[2] and Yulie Wu[1]

[1]*College of Mechatronics Engineering and Automation, National University of Defense Technology, Changsha 410073, China*

[2]*East China Institute of Photo-Electronic IC, Bengbu 233042, China*

(Received 12 July 2017; revised manuscript received 25 October 2017; published 29 December 2017)

This paper reports an alternative design strategy to reduce thermoelastic dissipation (TED) for isothermal-mode micromechanical resonators. This involves hanging lumped masses on a frame structure to decouple the resonant frequency and the effective beamwidth of the resonators, which enables the separation of the thermal relaxation rate and frequency of vibration. This approach is validated using silicon-based micromechanical disklike resonators engineered to isolate TED. A threefold improvement in the quality factor and a tenfold improvement in the decay-time constant is demonstrated. This work proposes a solution for isothermal-mode (flexural) micromechanical resonators to effectively mitigate TED. Specifically, this approach is ideal for designing high-performance gyroscope resonators based on microelectromechanical systems (MEMS) technology. It may pave the way for the next generation inertial-grade MEMS gyroscope, which remains a great challenge and is very appealing.

DOI: 10.1103/PhysRevApplied.8.064033

I. INTRODUCTION

Micro- and nanomechanical resonators have been widely used as front ends for ultrasensitive sensing, and precision measurements, such as chemical or biological sensing [1–6], wireless filters [7,8], frequency references [9], microscopy [10–12], inertial sensing [13–15], and many other applications [16–22]. The mechanical design of these small devices could greatly influence the overall performance of the instruments. A key figure of merit for a sensitive mechanical resonator is the quality factor (Q), which is defined as the ratio of the maximum strain energy to the dissipated energy per vibration cycle.

The relevant mechanical damping mechanisms of micro- and nanomechanical resonators have been extensively investigated. Some known damping mechanisms include air damping involving drag-force damping and squeeze-film air damping [23,24], material losses caused by defects in the bulk or on the surface of the resonator [25–28], clamping loss induced by energy transfer from the resonator to the substrate [29–31], and intrinsic damping in the resonator caused by phonon scattering (Akhiezer effect) [32–35] and phonon transport (i.e., thermoelastic dissipation, TED) [36–39]. These dissipation mechanisms are treated as dampers in parallel, such that the reciprocal of the overall Q value satisfies $Q^{-1} = \sum_j Q_j^{-1}$, where j labels the different mechanisms. Most damping mechanisms can be reduced by existing methods such as high-vacuum packaging, post-treatments, and anchoring resonators on nodes of vibration modes. Fundamental anharmonic effects caused by phonon interactions present fundamental upper limits of the Q value. Among them, TED is the dominating mechanism, especially in most flexural-mode resonators. Thus, the Q of many well-designed and well-fabricated micromechanical resonators is restricted by TED. TED is also an important damping factor in nanomechanical resonators at room temperature.

The intuitive picture of the TED process can be modeled based on classical heat transfer and the resulting entropy generation. TED has been known for a long time to be an important source of internal friction [40]. In recent years, TED has been revisited primarily because it is commonly encountered in micro- and nanomechanical devices. TED can be separated into two parts. The first part is material dependent, which determines the strength of the damping. The other part is both geometry and material dependent, which determines the frequency of peak damping. To reduce TED, materials should be selected that have a low thermal-expansion coefficient, and high thermal conductivity for isothermal-mode resonators or low thermal conductivity for adiabatic-mode resonators [41–43]. Moreover, structures with thin bending beams and low resonant frequencies for isothermal-mode resonators or thick bulk and high resonant frequencies for adiabatic-mode resonators should be designed. In particular, the mechanical design for a high thermoelastic quality factor (Q_{TED}) is a very tricky issue. The mechanical properties of micro- and nanoscale devices can impose ultimate limits on their performance, thus, the structural design can be of great significance. There are many examples of enhancing performance via innovative structural design or structural optimization of the micro- and nanomechanical devices [4,16,44–46]. For resonators

*dingbangxiao@nudt.edu.cn

working in the flexural mode, the key to designing a high-Q_{TED} structure is having a small beamwidth and low resonant frequency. Recently, great effort has been made to mitigate the TED of micromechanical resonators working in the flexural mode via structural refinement [47–49]. In most studies, the upper bound of Q_{TED} is confined by the coupling nature of the resonant frequency and the width of the bending beam (or the thermal relaxation rate). Thus, the resonant frequency cannot be further reduced once the beamwidth reaches its lower limit. Here, we introduce an alternative method to mitigate TED in the flexural mode by decoupling the resonant frequency and beamwidth. We demonstrate the efficacy of this approach by comparing Q_{TED}-enhanced microfabricated devices with conventional devices with similar structural parameters. The devices are engineered to isolate TED by greatly reducing other damping mechanisms.

II. RESULTS

A. TED mitigating design strategy

Sophisticated TED theoretical models that account for two-dimensional [38] or three-dimensional heat transfer [39] have been developed. Commercial finite-element-method software is able to estimate TED for complex structures. We use the classical one-dimensional TED model to reveal our TED-mitigating approach because of its explicitness. Moreover, the one-dimensional TED model has adequate precision for characterizing flexural-mode micro- and nanoresonators [50]. Because the majority of the heat transfer occurs in the thickness dimension in most flexural-mode cases.

The Lifshitz-Roukes model is a widely used exact one-dimensional TED theoretical model [36], based on which, Q_{TED} can be expressed by

$$Q_{\mathrm{TED}}^{-1} = \frac{E\alpha^2 T_0}{C}\left(\frac{6}{\xi^2} - \frac{6}{\xi^3}\frac{\sinh\xi + \sin\xi}{\cosh\xi + \cos\xi}\right), \qquad (1)$$

$$\xi = b\sqrt{\frac{C\pi f_0}{\kappa}}, \qquad (2)$$

where E is the Young's modulus, α is the linear coefficient of thermal expansion, T_0 is the equilibrium temperature, C is the specific heat per unit volume, b is the width of the bending beam, f_0 is the resonant frequency, and κ is the thermal conductivity of the material. Figure 1(a) shows that Q_{TED} of the single-crystal-silicon structures is a function of resonant frequency and beamwidth. For flexural-mode micro- and nanoresonators that demand a high Q_{TED}, it is much more preferable to work in the left side of the "valley," because it is more convenient for obtaining thinner beams and lower resonant frequency.

The conventional method of mitigating TED is to reduce the width of the bending beam. Because the beamwidth is directly coupled with the resonant frequency, the resonant frequency also decreases when reducing the beamwidth. However, this approach is limited, because the beamwidth cannot be infinitely small.

Here, we introduce an alternative approach to break this limitation. Our method is to hang lumped masses on frame structures by single beams to decouple the beamwidth and resonant frequency, as illustrated in Fig. 1(b). The resonant frequency f_0 is determined by the effective stiffness k_{eff} and effective mass m_{eff} of the resonator: $2\pi f_0 = \sqrt{k_{\mathrm{eff}}/m_{\mathrm{eff}}}$. Hanging lumped masses can greatly change m_{eff}, whereas it hardly affects k_{eff} [51]. This approach could provide a much lower resonant frequency and thus much lower ξ than conventional pure-frame structures. Moreover, this approach provides the capability of freely adjusting and controlling the resonant frequency or Q_{TED} independently from the width of the bending beam. Hanging lumped masses is feasible on the micro- and nanoscale because structures have much higher bending strength on these scales [52] and elastic deformation caused by gravity is negligible owing to the size effect.

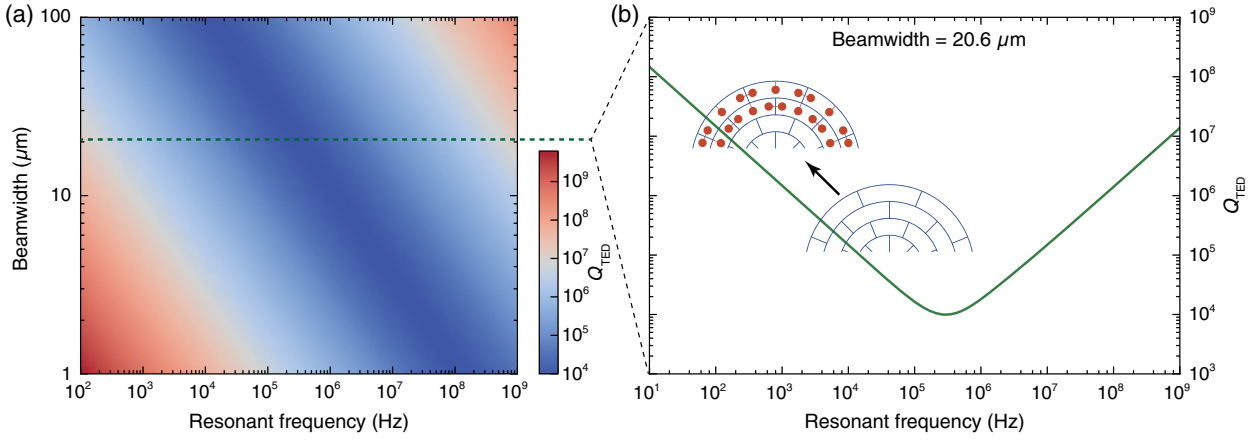

FIG. 1. (a) Thermoelastic quality-factor Q_{TED} as a function of resonant frequency and beamwidth. (b) Hanging lumped masses on frame structures by single beams to manipulate the resonant frequency independently of beamwidth, which can greatly enhance Q_{TED}.

The presented TED-mitigation approach can be explained based on the intuitionistic notion of thermal relaxation [36,40]. When the thermal relaxation rate f_{therm} is close to the frequency of vibration, the damping reaches a maximum value, where $f_{\text{therm}} = \kappa\pi^2/(Cb^2)$. Thus, the heart of mitigating TED is the separation of f_{therm} and the frequency of vibration. Our approach is to decouple f_{therm} from the resonant frequency f_0 of the resonators working under isothermal conditions, for which $f_0 \ll f_{\text{therm}}$. Thus, this method can provide an extra degree of freedom to manipulate TED beyond altering the beamwidth.

B. TED isolating design

To experimentally verify our approach, we have developed single-crystal-silicon-based disklike micromechanical resonators consisting of a symmetrical frame structure of 8-mm diameter and 150-μm height suspended by a central anchor with 4-mm diameter as depicted in Fig. 2. The flexible frame structure is made of nine concentrically nested, equally spaced rings connected with alternately spaced spokes. The rings and spokes have identical width, as shown in Fig. 2(a). The $b - f_0$ decoupling approach can be implemented by hanging lumped masses on the illustrated frame structures by single beams. In this study, the lumped masses are hung on the outer 2, 4, 6, and 8 layers of rings and spokes to vary the resonant frequency, as shown in Fig. 2(b). The structural parameters of the resonators are similar, as shown in Fig. 2(a). The resonators are actuated and transduced by capacitive electrodes. The capacitance gap is designed to be 15 μm. The devices are fabricated with an aligned Si-Si direct bonding and deep-reactive-ion-etching process. Photographs of the fabricated resonators are shown in Fig. 2(c).

The disklike design provides an ideal platform to isolate and study TED. First, the balanced wineglass operation modes greatly mitigate the clamping loss, as shown in Fig. 2(e). Second, appropriate dimensions of the micro-resonators provide very low effective surface-to-volume ratios, which results in a very small surface loss. In addition, these resonators are characterized in high-vacuum environments, in which air damping is also negligible, as shown in Fig. 2(f). To summarize, the disklike resonators can rule out the effect of additional critical damping mechanisms and hence isolate TED in the measured devices. In this study, we characterize the $n = 2$ wineglass modes of such resonators [see Fig. 2(d)]. We note that the $n = 2$ wineglass mode is the lowest balanced mode, which is more suitable for the one-dimension TED theory model than higher-order balanced modes. Moreover, the

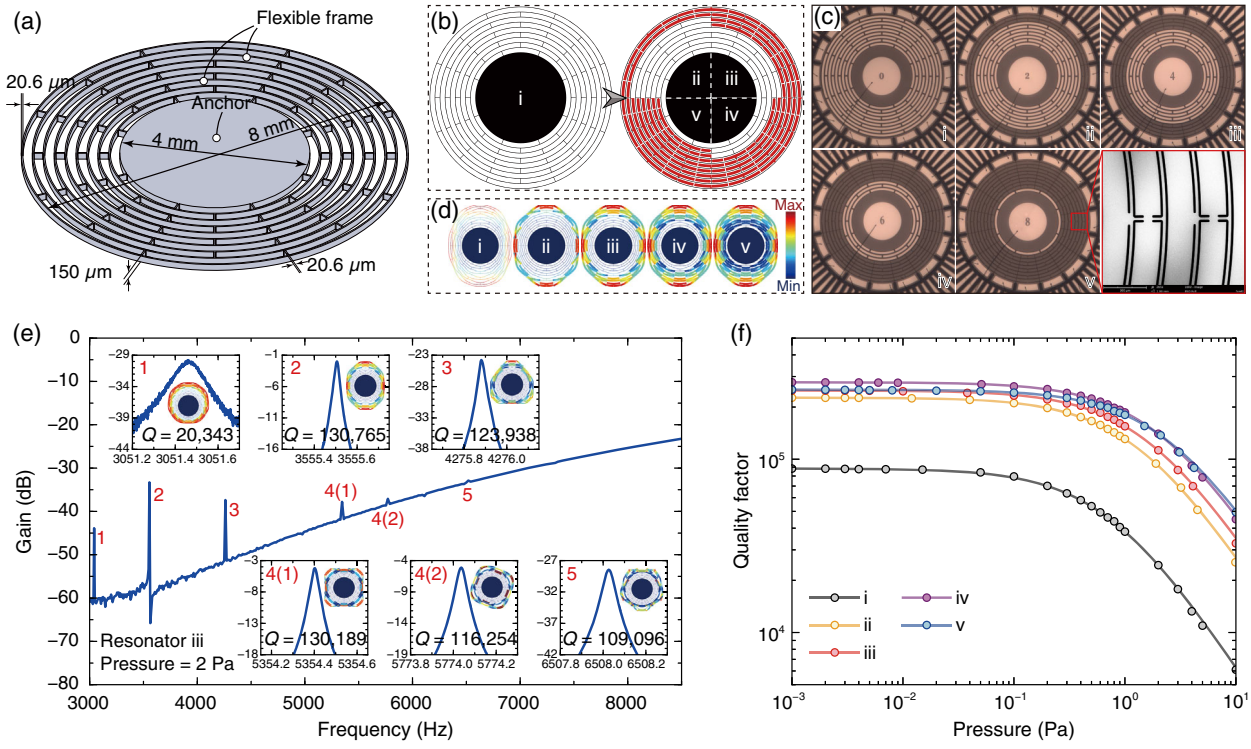

FIG. 2. (a) Dimensions of the frame structure of the disklike resonators. (b) Schematic of hanging lumped masses on the frame structure of the disklike resonators. Type i: frame-structure resonator. Types ii, iii, iv, and v: resonators with 2, 4, 6, and 8 outer layers of rings and spokes, respectively, hung with lumped masses. (c) Top-view photograph and a enlarged view of the fabricated resonators. (d) The $n = 2$ wineglass modes of the designed resonators. (e) Spectrum of a typical TED-isolating resonator (resonator iii) at room temperature and 2 Pa pressure. The $n = 2$ wineglass mode has the highest Q, which is used to study the TED. (f) Quality factors for resonators i, ii, iii, iv, and v when operated at various pressures. Q almost stops increasing when the pressure is below 0.01 Pa.

$n = 2$ wineglass mode is one of the most widely used balanced modes.

C. Verification

Dissipations of the TED-isolating disklike resonators are measured. The sample numbers of the different types of resonators are as follows: three type-i resonators, four type-ii resonators, three type-iii resonators, three type-iv resonators, and two type-v resonators. First, the spectrum method is used to find the $n = 2$ wineglass modes. Then, the ringdown method is used to precisely obtain Q. All dissipation measurements are performed at high vacuum (10^{-3} Pa) and at room temperature (300 K). Air damping is suppressed under these conditions. Based on the pressure–quality-factor curve, Q_{air} of each kind of resonator under 0.001 Pa can be calculated [53]. The recorded decaying signal is filtered, normalized, and enveloped. The decay-time constant τ is calculated by fitting the envelope with an inverse exponential function, $A_0 \exp(-t/\tau)$, where t is the time. Q is then calculated based on $Q = \pi f_0 \tau$. The tested results are illustrated in Fig. 3(a) and summarized in Table I. Figure 3(b) shows the highest-tested Q of resonators i–v. The maximum and minimum Q of the pure-frame resonator (type i) are 88 291 and 78 132, respectively. The Q of the $b - f_0$ decoupled resonators (types ii–v) ranges from 195 274 to 277 924, with the minimum Q being observed from resonator ii (i.e., with two outer layers of rings and spokes hung with lumped masses) and the maximum Q is observed from resonator iv (i.e., with six outer layers of rings and spokes hung with lumped masses). To further enhance the effectiveness of the design strategy, data from one more disklike resonator reported in Ref. [51] is also included in Fig. 3. The basic structural parameters of this resonator are similar to those of resonators i–v, whereas the five outer layers of rings are interconnected with 16 rather than eight spokes, and the outer four layers of rings and spokes are hung with lumped masses. It provides higher stiffness and thus higher resonant frequency than resonators i–v. The tested resonant frequency and Q of the $n = 2$ wineglass mode are 5770 and 157 508 Hz, respectively. The results coincide well with the theoretical expectation, as shown in Fig. 3(a). We estimate Q_{TED}'s of the resonators using the one-dimensional Lifshitz-Roukes model by substituting the measured beamwidth (20.6 μm) and the tested resonant frequencies of each resonator into Eqs. (1) and (2). The simulated values based on the three-dimensional TED theory are generated using the geometric parameters determined via a careful measurement of the fabricated resonators. The calculated and simulated Q_{TED} of each resonator are also shown in Fig. 3(a).

Figure 3 reveals some interesting features. First, the $b - f_0$ decoupled resonators provide much higher Q and lower f_0 than the pure-frame resonators. Because the TED-isolating resonators are dominated by TED, it can be inferred that the $b - f_0$ decoupling approach greatly mitigates the TED in these resonators. This is also reflected in the TED simulation results. Second, there is a disparity in the trends of the one-dimensional and three-dimensional models. The reason for this is that the one-dimensional TED model only considers the irreversible heat flow across the beam thickness, whereas the three-dimensional model also accounts for the heat flows along the longitudinal and height axes. Moreover, the one-dimensional TED model leaves out the structural boundary conditions and mode shapes of the resonator, whereas the three-dimensional

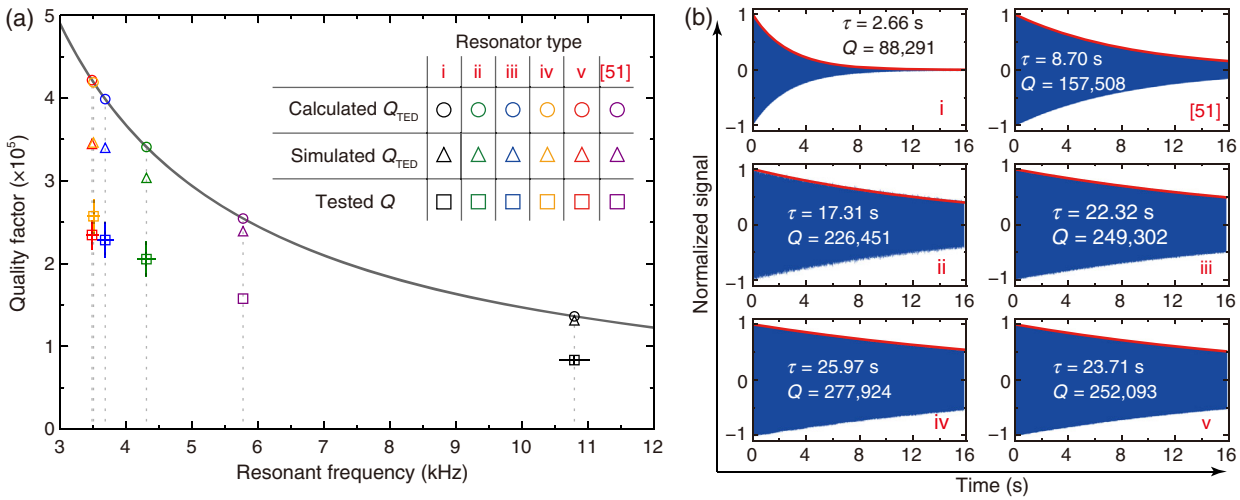

FIG. 3. Quality-factor comparison between the $b - f_0$ decoupled disklike resonators and the pure-frame resonators. (a) Calculated Q_{TED}'s based on the one-dimensional Lifshitz-Roukes TED model, simulated Q_{TED}'s using COSMOL Multiphysics (which is based on a three-dimensional TED model), and experimentally tested Qs of resonators i–v. The Qs are tested based on the ringdown method. An additional disklike resonator reported in Ref. [51] is also included. (b) The best experimental results of each kind of resonator. The red line is the fitted envelope of the decaying signal.

TABLE I. Basic properties of the TED isolating disklike resonators.

	f_0 (Hz)		τ (s)		Tested Q				
Resonator type	Max	Min	Max	Min	Max	Min	Calculated Q_{TED}[a]	Simulated Q_{TED}[b]	Q_{air}
i	11 030	10 561	2.66	2.26	88 291	78 132	136 100	131 300	67×10^6
ii	4446	4164	17.31	14.29	226 451	195 274	340 900	303 600	307×10^6
iii	3805	3556	22.32	17.35	249 302	207 391	398 700	339 900	408×10^6
iv	3599	3406	25.97	20.90	277 924	236 244	418 900	346 300	564×10^6
v	3576	3383	23.71	19.29	252 093	216 783	421 600	344 600	630×10^6

[a]Calculated based on the one-dimensional Lifshitz-Roukes TED model.
[b]Simulated using COMSOL Multiphysics, which is based on the three-dimensional TED model.

model takes into account the mode shapes and the majority of boundary conditions. The structures and the $n = 2$ wineglass mode shapes of the TED-isolating resonators are complex. Therefore, the TED calculation based on the one-dimensional TED model may not be as precise as that based on the three-dimensional one. Third, both simulations and experiments demonstrate that although the resonator with eight layers of masses (i.e., resonator v) has the lowest f_0, it provides a lower Q_{TED} and Q than the resonator with six layers (i.e., resonator iv). This is a representative example of the divergence of the one-dimensional and three-dimensional TED models. Our explanation is as follows. It is mostly the change of the effective mass m_{eff} that modifies f_0 when adding lumped masses. The effective mass is defined as $m_{\mathrm{eff}} = \lambda M$, where M is the real mass, and λ is a coefficient smaller than 1, which is determined by

$$\lambda = \frac{\iiint_V x^2/q^2 dV}{\iiint_V 1 dV}. \tag{3}$$

Here, x is the displacement of each mass point, and q is the amplitude (maximum $|x|$). The displacements of the resonator's inner rings and spokes are relatively small compared with the outer ones. Thus, when adding a lumped mass in the inner rings and spokes, m_{eff} of the overall resonator changes only slightly. Accordingly, there is only a small change in m_{eff} and f_0 of resonator v compared with resonator iv. However, hanging lumped masses on the rings and spokes may to some degree increase the equivalent thickness of the beams across which heat conduction occurs. If lumped masses are added on the inner rings and spokes, the increase of equivalent thickness prevails over the reduction of f_0, which leads to an exacerbation of TED. Last, if the measured data are fitted with the model of $Q^{-1} = Q_{\mathrm{TED}}^{-1} + Q_{\mathrm{air}}^{-1} + Q_{\mathrm{other}}^{-1}$, we will find that the unknown Q_{other} is frequency dependent, and Q_{other} increases when f_0 reduces, which is very like the characteristic of the TED. The rational hypothesis is that the simulated Q_{TED} is higher than the actual Q_{TED} of the fabricated resonators. Thus, some residual TED is still included in the calculated Q_{other}^{-1}.

III. DISCUSSION

Although the $b - f_0$ decoupling design strategy is verified using micromechanical resonators to exclude the surface dissipation, it may also be instructive for designing nanomechanical resonators, because TED is a very important damping mechanism on the nanoscale as well. This method can also be widely applied to other types of flexural resonators, such as doubly clamped beams [54,55], cantilevers [56], free-free beams [29], rings [57–59], tuning forks [60,61], etc. It is also feasible for enhancing the Q_{TED} of resonators made from other high-thermal-conductivity materials other than single-crystal silicon (such as diamond, GaN, and SiC). In addition, this method may lead to a change in the overall design strategy for isothermal-mode micromechanical resonators, and it may also provide an alternative perspective for the design of some nanomechanical resonators.

More importantly, this TED-mitigation method may pave the way for making an inertial-grade [62] microelectromechanical systems (MEMS) Coriolis vibratory gyroscope (CVG), which remains a great challenge and is very appealing. The bias and bias drift of the common force-to-rebalance mode MEMS CVG is scaled by a figure of merit (FOM) defined by $\mathrm{FOM} = 1/(2A_g\tau)$ [63], where A_g is the angular gain factor determined by the mode shape of the resonator. Our method can be used to engineer very long τ to depress the bias and drift to the inertial grade. Moreover, if the transducers are appropriately designed, the greatly improved mechanical sensitivity [46] of the MEMS CVG, owing to the increase of τ, may result in an impressive enhancement for the signal-to-noise ratio. Last but not least, the mechanical resolution of the resonator can also be improved using this strategy. Brownian noise provides a theoretical lower limit for gyroscope resolution, which is given by $\Omega_{\mathrm{Brown}} = \sqrt{k_B T/(2k_{\mathrm{eff}}\tau)}/(A_g x_0)$ [57,64], where k_B, T, and x_0 are the Boltzmann's constant, temperature, and mechanical amplitude of the driving mode, respectively. τ is greatly improved and the other parameters are almost unaffected in our method. Thus, the Brownian noise can be greatly depressed. Overall, this TED-mitigation method may have a notable impact on the

MEMS CVG resonator design. In particular, the τ enhancement demonstrated in this paper may produce an order-of-magnitude promotion in bias stability and severalfold enhancement in mechanical resolution, which could strike some of the most sophisticated tactical-grade MEMS CVGs [13,14,63] into inertial grade.

The highest Q and τ of the $b - f_0$ decoupled resonator with a beamwidth of 20.6 μm is demonstrated to be 277 924 and 25.97 s, respectively. These are record values for silicon resonators with a similar beamwidth. A higher Q could be obtained if the lumped masses were further increased or if this approach were applied to resonators with thinner beams.

As concise theory, the one-dimensional TED model may have some degree of error in calculating Q_{TED} of complex structures and high-order modes. However, it is still quite rational for estimating and qualitatively comparing Q_{TED} of conventional resonators. When utilizing the $b - f_0$ decoupling design method, it is advisable to add lumped masses in positions that have relatively large displacement.

IV. CONCLUSION

In conclusion, we have presented an alternative design strategy of hanging lumped masses on a frame structure to mitigate TED of micromechanical flexural resonators made from high-thermal-conductivity materials. The heart of this design method is decoupling the resonant frequency from the effective beamwidth (or the thermal relaxation rate). Our approach has been validated using TED-isolating MEMS resonators. The $b - f_0$ decoupling method provides a universal way to engineer high Q_{TED}. It could be very constructive for enhancing the sensitivity, resolution, and stability of micromechanical resonating sensor systems. The application of this method to the next-generation MEMS gyroscope has been elaborated.

ACKNOWLEDGMENTS

This work has been supported by the National Natural Science Foundation of China under Grant No. 51575521. The authors thank Prof. Zhihua Chen, Dr. Xinghua Wang, Dr. Huacheng Qiu, Dr. Xiang Xi, Dr. Jian Zhou, and Dr. Bin Yu at National University of Defense Technology for their helpful discussions. The authors also thank Qunying Guo and Dongfang Song at East China Institute of Photo-Electronic IC for their assistance in device fabrication.

[1] Mo Li, H. X. Tang, and M. L. Roukes, Ultra-sensitive NEMS-based cantilevers for sensing, scanned probe and very high-frequency applications, Nat. Nanotechnol. **2**, 114 (2007).

[2] M. S. Hanay, S. Kelber, A. K. Naik, D. Chi, S. Hentz, E. C. Bullard, E. Colinet, L. Duraffourg, and M. L. Roukes, Single-protein nanomechanical mass spectrometry in real time, Nat. Nanotechnol. **7**, 602 (2012).

[3] Jérôme Charmet, Thomas C. T. Michaels, Ronan Daly, Abhinav Prasad, Pradyumna Thiruvenkathanathan, Robin S. Langley, Tuomas P. J. Knowles, and Ashwin A. Seshia, Quantifying Measurement Fluctuations from Stochastic Surface Processes on Sensors with Heterogeneous Sensitivity, Phys. Rev. Applied **5**, 064016 (2016).

[4] Kidong Park, Larry J. Millet, Namjung Kim, Huan Li, Xiaozhong Jin, Gabriel Popescu, N. R. Aluru, K. Jimmy Hsia, and Rashid Bashir, Measurement of adherent cell mass and growth, Proc. Natl. Acad. Sci. U.S.A. **107**, 20691 (2010).

[5] Jinsung Park, Doyeon Bang, Kuewhan Jang, Eunkyoung Kim, Seungjoo Haam, and Sungsoo Na, Multimodal label-free detection and discrimination for small molecules using a nanoporous resonator, Nat. Commun. **5**, 3456 (2014).

[6] Larry J. Millet, Elise A. Corbin, Robert Free, Kidong Park, Hyunjoon Kong, William P. King, and Rashid Bashir, Characterization of mass and swelling of hydrogel microstructures using MEMS resonant mass sensor arrays, Small **8**, 2555 (2012).

[7] C. T. C. Nguyen, Frequency-selective MEMS for miniaturized low-power communication devices, IEEE Trans. Microwave Theory Tech. **47**, 1486 (1999).

[8] J. R. Clark, W. T. Hsu, M. A. Abdelmoneum, and C. T. C. Nguyen, High-Q UHF micromechanical radial-contour mode disk resonators, J. Microelectromech. Syst. **14**, 1298 (2005).

[9] Clark T. C. Nguyen, MEMS technology for timing and frequency control, IEEE Trans. Ultrason. Ferroelectr. Freq. Control **54**, 251 (2007).

[10] G. Binnig, C. F. Quate, and Ch. Gerber, Atomic Force Microscope, Phys. Rev. Lett. **56**, 930 (1986).

[11] C. L. Degen, M. Poggio, H. J. Mamin, C. T. Rettner, and D. Rugar, Nanoscale magnetic resonance imaging, Proc. Natl. Acad. Sci. U.S.A. **106**, 1313 (2009).

[12] Michael G. Ruppert, Anthony G. Fowler, Mohammad Maroufi, and S. O. Reza Moheimani, On-chip dynamic mode atomic force microscopy: A silicon-on-insulator MEMS approach, J. Microelectromech. Syst. **26**, 215 (2017).

[13] Sarah H. Nitzan, Valentina Zega, Mo Li, Chae H. Ahn, Alberto Corigliano, Thomas W. Kenny, and David A. Horsley, Self-induced parametric amplification arising from nonlinear elastic coupling in a micromechanical resonating disk gyroscope, Sci. Rep. **5**, 9036 (2015).

[14] C. H. Ahn, S. Nitzan, E. J. Ng, V. A. Hong, Y. Yang, T. Kimbrell, D. A. Horsley, and T. W. Kenny, Encapsulated high frequency (235 kHz), high-Q (100 k) disk resonator gyroscope with electrostatic parametric pump, Appl. Phys. Lett. **105**, 243504 (2014).

[15] D. Yamane, T. Konishi, T. Matsushima, K. Machida, H. Toshiyoshi, and K. Masu, Design of sub-1g microelectromechanical systems accelerometers, Appl. Phys. Lett. **104**, 074102 (2014).

[16] R. P. Middlemiss, A. Samarelli, D. J. Paul, J. Hough, S. Rowan, and G. D. Hammond, Measurement of the earth tides with a MEMS gravimeter, Nature (London) **531**, 614 (2016).

[17] A. D. O'Connell, M. Hofheinz, M. Ansmann, Radoslaw C. Bialczak, M. Lenander, Erik Lucero, M. Neeley, D. Sank, H. Wang, M. Weides, J. Wenner, John M. Martinis, and

A. N. Cleland, Quantum ground state and single-phonon control of a mechanical resonator, Nature (London) **464**, 697 (2010).

[18] Shimon Kolkowitz, Ania C. Bleszynski Jayich, Quirin P. Unterreithmeier, Steven D. Bennett, Peter Rabl, J. G. E. Harris, and Mikhail D. Lukin, Coherent sensing of a mechanical resonator with a single-spin qubit, Science **335**, 1603 (2012).

[19] J.-M. Pirkkalainen, E. Damskägg, M. Brandt, F. Massel, and M. A. Sillanpää, Squeezing of Quantum Noise of Motion in a Micromechanical Resonator, Phys. Rev. Lett. **115**, 243601 (2015).

[20] S. Etaki, F. Konschelle, Ya M. Blanter, H. Yamaguchi, and H. S. J. van der Zant, Self-sustained oscillations of a torsional SQUID resonator induced by Lorentz-force back-action, Nat. Commun. **4**, 1803 (2013).

[21] D. A. Garanin and E. M. Chudnovsky, Quantum Entanglement of a Tunneling Spin with Mechanical Modes of a Torsional Resonator, Phys. Rev. X **1**, 011005 (2011).

[22] K. C. Schwab and M. L. Roukes, Putting mechanics into quantum mechanics, Phys. Today **58**, No. 7, 36 (2005).

[23] M. H. Bao, H. Yang, H. Yin, and Y. C. Sun, Energy transfer model for squeeze-film air damping in low vacuum, J. Micromech. Microeng. **12**, 341 (2002).

[24] J. F. Vignola, J. A. Judge, J. Jarzynski, M. Zalalutdinov, B. H. Houston, and J. W. Baldwin, Effect of viscous loss on mechanical resonators designed for mass detection, Appl. Phys. Lett. **88**, 041921 (2006).

[25] P. Mohanty, D. A. Harrington, K. L. Ekinci, Y. T. Yang, M. J. Murphy, and M. L. Roukes, Intrinsic dissipation in high-frequency micromechanical resonators, Phys. Rev. B **66**, 085416 (2002).

[26] Quirin P. Unterreithmeier, Thomas Faust, and Jörg P. Kotthaus, Damping of Nanomechanical Resonators, Phys. Rev. Lett. **105**, 027205 (2010).

[27] C. Seoánez, F. Guinea, and A. H. Castro Neto, Surface dissipation in nanoelectromechanical systems: Unified description with the standard tunneling model and effects of metallic electrodes, Phys. Rev. B **77**, 125107 (2008).

[28] K. Y. Yasumura, T. D. Stowe, E. M. Chow, T. Pfafman, T. W. Kenny, B. C. Stipe, and D. Rugar, Quality factors in micron- and submicron-thick cantilevers, J. Microelectromech. Syst. **9**, 117 (2000).

[29] Garrett D. Cole, Ignacio Wilson-Rae, Katharina Werbach, Michael R. Vanner, and Markus Aspelmeyer, Phonon-tunnelling dissipation in mechanical resonators, Nat. Commun. **2**, 231 (2011).

[30] Johannes Rieger, Andreas Isacsson, Maximilian J. Seitner, Joerg P. Kotthaus, and Eva M. Weig, Energy losses of nanomechanical resonators induced by atomic force microscopy—Controlled mechanical impedance mismatching, Nat. Commun. **5**, 3345 (2014).

[31] Ali Darvishian, Behrouz Shiari, Jae Yoong Cho, Tal Nagourney, and Khalil Najafi, Anchor loss in hemispherical shell resonators, J. Microelectromech. Syst. **26**, 51 (2017).

[32] A. A. Kiselev and G. J. Iafrate, Phonon dynamics and phonon assisted losses in Euler-Bernoulli nanobeams, Phys. Rev. B **77**, 205436 (2008).

[33] K. Kunal and N. R. Aluru, Akhiezer damping in nanostructures, Phys. Rev. B **84**, 245450 (2011).

[34] Shirin Ghaffari, Saurabh A. Chandorkar, Shasha Wang, Eldwin J. Ng, Chae H. Ahn, Vu Hong, Yushi Yang, and Thomas W. Kenny, Quantum limit of quality factor in silicon micro and nano mechanical resonators, Sci. Rep. **3**, 3244 (2013).

[35] Srikanth S. Iyer and Robert N. Candler, Mode- and Direction-Dependent Mechanical Energy Dissipation in Single-Crystal Resonators due to Anharmonic Phonon-Phonon Scattering, Phys. Rev. Applied **5**, 034002 (2016).

[36] Ron Lifshitz and M. L. Roukes, Thermoelastic damping in micro- and nanomechanical systems, Phys. Rev. B **61**, 5600 (2000).

[37] Sudipto K. De and N. R. Aluru, Theory of thermoelastic damping in electrostatically actuated microstructures, Phys. Rev. B **74**, 144305 (2006).

[38] Sairam Prabhakar and Srikar Vengallatore, Theory of thermoelastic damping in micromechanical resonators with two-dimensional heat conduction, J. Microelectromech. Syst. **17**, 494 (2008).

[39] Saurabh A. Chandorkar, Robert N. Candler, Amy Duwel, Renata Melamud, Manu Agarwal, Kenneth E. Goodson, and Thomas W. Kenny, Multimode thermoelastic dissipation, J. Appl. Phys. **105**, 043505 (2009).

[40] C. Zener, Internal friction in solids II. General theory of thermoelastic internal friction, Phys. Rev. **53**, 90 (1938).

[41] Y. Tao, J. M. Boss, B. A. Moores, and C. L. Degen, Single-crystal diamond nanomechanical resonators with quality factors exceeding one million, Nat. Commun. **5**, 3638 (2014).

[42] Hadi Najar, Amir Heidari, Mei-Lin Chan, Hseuh-An Yang, Liwei Lin, David G. Cahill, and David A. Horsley, Microcrystalline diamond micromechanical resonators with quality factor limited by thermoelastic damping, Appl. Phys. Lett. **102**, 071901 (2013).

[43] Hadi Najar, Mei-Lin Chan, Hsueh-An Yang, Liwei Lin, David G. Cahill, and David A. Horsley, High quality factor nanocrystalline diamond micromechanical resonators limited by thermoelastic damping, Appl. Phys. Lett. **104**, 151903 (2014).

[44] Menno Poot and Herre S. J. van der Zant, Mechanical systems in the quantum regime, Phys. Rep. **511**, 273 (2012), mechanical systems in the quantum regime.

[45] Rob N. Candler, Amy Duwel, Mathew Varghese, Saurabh A. Chandorkar, Matthew A. Hopcroft, Woo-Tae Park, Bongsang Kim, Gary Yama, Aaron Partridge, Markus Lutz, and Thomas W. Kenny, Impact of geometry on thermoelastic dissipation in micromechanical resonant beams, J. Microelectromech. Syst. **15**, 927 (2006).

[46] Xin Zhou, Dingbang Xiao, Zhanqiang Hou, Qingsong Li, Yulie Wu, and Xuezhong Wu, Influences of the structure parameters on sensitivity and Brownian noise of the disk resonator gyroscope, J. Microelectromech. Syst. **26**, 519 (2017).

[47] Amy Duwel, Rob N. Candler, Thomas W. Kenny, and Mathew Varghese, Engineering MEMS resonators with low thermoelastic damping, J. Microelectromech. Syst. **15**, 1437 (2006).

[48] Jonathan James Lake, Amy Elizabeth Duwel, and Rob N. Candler, Particle swarm optimization for design of slotted MEMS resonators with low thermoelastic dissipation, J. Microelectromech. Syst. **23**, 364 (2014).

[49] Dustin D. Gerrard, Chae H. Ahn, Ian B. Flader, Yunhan Chen, Eldwin J. Ng, Yushi Yang, and Thomas W. Kenny, *Q*-factor optimization in disk resonator gyroscopes via geometric parameterization, in *Proceedings of the 2016 IEEE 29th International Conference on Micro Electro Mechanical Systems (MEMS)* (IEEE, New York, 2016), pp. 994–997.

[50] Xin Zhou, Dingbang Xiao, Zhanqiang Hou, Qingsong Li, Yulie Wu, Dechuan Yu, Wei Li, and Xuezhong Wu, Thermoelastic quality-factor enhanced disk resonator gyroscope, in *Proceedings of the 30th IEEE International Conference on Micro Electro Mechanical Systems (MEMS 2017)* (IEEE, New York, 2017), pp. 1009–1012.

[51] Xin Zhou, Dingbang Xiao, Xuezhong Wu, Yulie Wu, Zhanqiang Hou, Kaixuan He, and Qingsong Li, Stiffness-mass decoupled silicon disk resonator for high resolution gyroscopic application with long decay time constant (8.695 s), Appl. Phys. Lett. **109**, 263501 (2016).

[52] T. Namazu, Y. Isono, and T. Tanaka, Evaluation of size effect on mechanical properties of single crystal silicon by nanoscale bending test using AFM, J. Microelectromech. Syst. **9**, 450 (2000).

[53] Bongsang Kim, Matthew A. Hopcroft, Rob N. Candler, Chandra Mohan Jha, Manu Agarwal, Renata Melamud, Saurabh A. Chandorkar, Gary Yama, and Thomas W. Kenny, Temperature dependence of quality factor in MEMS resonators, J. Microelectromech. Syst. **17**, 755 (2008).

[54] H. J. R. Westra, M. Poot, H. S. J. van der Zant, and W. J. Venstra, Nonlinear Modal Interactions in Clamped-Clamped Mechanical Resonators, Phys. Rev. Lett. **105**, 117205 (2010).

[55] Changyao Chen, Damian Zanette, David Czaplewski, Jeffrey Guest, Steve Shaw, Mark Dykman, and Daniel Lopez, Direct observation of coherent energy transfer in nonlinear micromechanical oscillators, Nat. Commun. **8**, 15523 (2017).

[56] Yu Jia and Ashwin A. Seshia, Power optimization by mass tuning for MEMS piezoelectric cantilever vibration energy harvesting, J. Microelectromech. Syst. **25**, 108 (2016).

[57] F Ayazi and K Najafi, A HARPSS polysilicon vibrating ring gyroscope, J. Microelectromech. Syst. **10**, 169 (2001).

[58] S. J. Wong, C. H. J. Fox, S Mcwilliam, C. P. Fell, and R. Eley, A preliminary investigation of thermo-elastic damping in silicon rings, J. Micromech. Microeng. **14**, S108 (2004).

[59] B. J. Gallacher, J. Hedley, J. S. Burdess, A. J. Harris, A. Rickard, and D. O. King, Electrostatic correction of structural imperfections present in a microring gyroscope, J. Microelectromech. Syst. **14**, 221 (2005).

[60] D. K. Agrawal, J. Woodhouse, and A. A. Seshia, Observation of Locked Phase Dynamics and Enhanced Frequency Stability in Synchronized Micromechanical Oscillators, Phys. Rev. Lett. **111**, 084101 (2013).

[61] Pavel M. Polunin, Yushi Yang, Mark I. Dykman, Thomas W. Kenny, and Steven W. Shaw, Characterization of MEMS resonator nonlinearities using the ringdown response, J. Microelectromech. Syst. **25**, 297 (2016).

[62] N. Yazdi, F. Ayazi, and K. Najafi, Micromachined inertial sensors, Proc. IEEE **86**, 1640 (2002).

[63] Anthony D. Challoner, Howard H. Ge, and John Y. Liu, *Boeing disc resonator gyroscope, in Position, Location and Navigation Symposium—PLANS 2014, 2014 IEEE/ION* (IEEE, New York, 2014), pp. 504–514.

[64] R. P. Leland, Mechanical-thermal noise in MEMS gyroscopes, IEEE Sens. J. **5**, 493 (2005).